https://doi.org/10.3311/PPci.16790

Periodica Polytechnica Civil Engineering, 65(1), pp. 1–14, 2021

Factors in the Relationship Between Optimal CO_2 Emission and Optimal Cost of the RC Frames

Lida Mottaghi[1], Ramezan Ali Izadifard[1], Ali Kaveh[2*]

[1] Department of Civil Engineering, Imam Khomeini International University, 34148-96818 Qazvin, Iran
[2] Centre of Excellence for Fundamental Studies in Structural Engineering, School of Civil Engineering, Iran University of Science and Technology, Narmak, Tehran-16, Iran
* Corresponding author, e-mail: alikaveh@iust.ac.ir

Received: 06 July 2020, Accepted: 06 August 2020, Published online: 17 September 2020

Abstract

Nowadays, reduction of greenhouse gases emissions from the construction industry is seriously under investigation. The aim of this study is to investigate the various effective factors on the relationship between optimal cost and optimal carbon dioxide emissions of the reinforced concrete structures with nonlinear structural behavior. A four-story reinforced concrete frame is designed for various peak ground accelerations (PGAs) and all ductility classes according to Iran's seismic resistant design-2800 code, as well as for different concrete classes. The frames are optimally designed according to ACI 318-08 and FEMA codes. The results of optimal designs show that the design of structures with medium and high ductility class produces less cost and CO_2 emissions than the low ductility class. On the other hand, the relationship between cost and CO_2 emissions shows that in the low ductility class, increasing the percentage of the optimal cost can greatly reduce the amount of CO_2 emissions. PGA design has a significant effect on reducing optimal cost and CO_2 emissions. Especially in the low ductility class, reducing this parameter can greatly decrease the amount of the objective functions. Also, the use of concrete with low class can reduce the cost and CO_2 emissions but the effect of this parameter in the objective is very small.

Keywords

RC frame, performance-based seismic design, optimal cost, optimal CO_2 emissions, ECBO algorithm, influence factors

1 Introduction

In the optimal design of structures, the objective is minimizing the consumed material while satisfying the constraints based on design codes. In most studies of steel frames, minimizing the weight structures has been considered [1–3] also, in many researches on concrete frames, the aim is to minimize the material costs [4–9]. On the other hand, nowadays reduction of greenhouse gas has become a major global challenge. On average, 40 % of the total global energy consumption are from the construction industry. This energy consumption of the building has increased greenhouse gases. Reinforced concrete buildings contribute to the environmental impact due to CO_2 emissions during the production of cement and reinforcing steel. Many studies have examined strategies to reduce CO_2 emissions in the design of concrete buildings. Some studies have suggested the use of new materials such as low-carbon concrete [10, 11]. In other studies, optimization techniques are used to minimize CO_2 emissions during structural design. Due to the fact that RC structures are composed of two heterogeneous materials, concrete and steel, and these materials produce different amounts of carbon dioxide, so the problem has a good potential in the optimization method. Eleftheriadis et al. [12] presented a method for optimizing the cost and CO_2 emissions in reinforced concrete buildings based on BIM. In which the multilevel engineering analysis model has been used to optimize the structures, including 1) structural layout, 2) the size of slab and columns, 3) the bars of columns and slab. Yoon et al. [13] have described a process for optimizing the embodied energy, CO_2 emissions and the cost of reinforced concrete columns. Therefore, a short reinforced concrete column with a square cross section under different axial and bending loads was investigated. Their study showed that in general, the objective function of cost can be reduced by reducing the amount of steel. But the objective function of CO_2 emissions can be effectively reduced by reducing the amount of concrete. Compared to the cost and CO_2 emission, embodied energy is affected by both the

Cite this article as: Mottaghi, L., Izadifard, R. A., Kaveh, A. "Factors in the Relationship Between Optimal CO_2 Emission and Optimal Cost of the RC Frames", Periodica Polytechnica Civil Engineering, 65(1), pp. 1–14, 2021. https://doi.org/10.3311/PPci.16790

amount of concrete and steel reinforcement. de Medeiros et al. [14] used a harmony search algorithm to minimize the monetary and environmental costs of the rectangular reinforced concrete columns, subjected to compressive and flexural pressures. In addition to material costs, environmental impacts such as carbon dioxide emissions, global warming potential (GWP), energy consumption, and environmental scoring units, known as the Eco Index, have also been investigated. Park et al. [15]examined the effects of design factors (concrete strength, steel reinforcement strength, cross-section size, and amount of steel reinforcement) on CO_2 emissions and cost of the RC column and showed that increasing the strength and amount of steel reinforcements is effective for sustainable design. Increasing the strength and amount of the concrete is effective for economical design. Camp et al. [16] are optimally designed the RC frame with the aim of minimizing cost and CO_2 emissions using a big bang-big crunch algorithm. They showed that by increasing the small amount of optimal cost, optimal carbon dioxide emissions can be reduced. Paya-Zaforteza et al. [17] used the simulated annealing (SA) algorithm to minimize embedded CO_2 emissions and the economic cost of RC frame. Kaveh et al. [18] investigated the trade-offs between optimal cost and optimal CO_2 emissions of the reinforced concrete frames with three metaheuristic algorithms. In another study, they extended their studies to optimal design of RC frames with non-prismatic beams [19]. In addition, Kaveh and Ardalani [20] developed a computational procedure to obtained pareto results of the objective function of cost and CO_2 emissions by using NSECBO algorithm. Park et al. [21] developed an integrated analysis model for minimizing of carbon dioxide emissions, seismic performance, and costs of RC frames through performance-based optimal seismic design. Mergos [22] has identified efficient design methods that minimize the environmental impact of seismic resistant frames. In which a three-story two-span RC frame is optimally designed for all ductility classes according EC8 and for various design peak ground accelerations (PGAs), concrete classes and material embodied CO_2 footprint scenarios. He used equivalent static linear analysis to calculate the seismic response of the frame and used the genetic algorithm for design of frame. In his work the dimensions of beams, columns and steel reinforcement were considered as variables.

A review of the literature shows that only a limited number of studies have been conducted on the trade-offs between optimal cost and optimal carbon dioxide in seismic design of reinforced concrete structures, where nonlinear analysis being used for the analysis of the structures. In this study, a four-story two-span reinforced concrete frame is designed for all ductility classes and various peak ground accelerations according Iran's seismic resistant design-2800 code [23], various concrete classes. Here, ECBO algorithm is used for optimal design. The relationship between cost and carbon dioxide emissions is investigated in optimal designs. Nonlinear static analysis is used to analyze the structure. In which, the seismic responses of the structure are obtained under linear static analysis and serviceability constraints are controlled, then the structure is modeled with nonlinear behavior and analyzed under nonlinear static analysis, and finally the performance limit states are controlled.

2 Formulation of optimal design

The procedure used for performance based optimal seismic design as well as the constraints associated with this design are adopted from the previous papers of the authors.

2.1 Performance-based optimum seismic design (PBOSD)

The procedure of PBOSD for problem is formulated as Eq. (1). Linear equivalent static analysis is performed for structures and the serviceability constraints are checked according ACI 318-08 code [24]. Then, nonlinear static analysis are performed according to FEMA-273 [25]and the maximum inter-story drift are checked.

$$\begin{cases} min\ f(x) \\ \quad g_j^{SERV} \qquad j=1,\ldots,m \\ \quad g_j^{PBD} \qquad j=1,\ldots,k \\ \quad x^L \le x \le x^U \end{cases} \tag{1}$$

The load combinations Eq. (2) according to the ACI 318-08 code, are used for equivalent static analysis. Where, D is the dead load and L is the live load. The live and dead loads are considered as 10.7 kN/m and 22.3 kN/m, respectively. Seismic lateral load (E) is calculated according 2800 code for all ductility classes and various PGA.

$$Q_G^{serv} = \begin{cases} 1.2D + 1.6L \\ 1.2D + L \pm 1.4E \\ 0.9D \pm 1.4E \end{cases} \tag{2}$$

In nonlinear static analysis the combination of gravity load according to FEMA-273 Eq. (3) and lateral load based with load pattern first mode are used. The gravity load is

applied constantly, and lateral load is applied incrementally until the displacement of the roof either reaches to target displacement or mathematical instability occurs. According to FEMA-356 [26] the target displacement is calculated as Eq. (4).

$$Q_G^{PBD} = 1.1\left(D + L\right) \tag{3}$$

$$\delta t = C_0 C_1 C_2 C_3 S_a \frac{Te^2}{4\pi^2} g \tag{4}$$

Where the C_0 is the modification factor for relating the spectral displacement of a single degree of freedom to the roof of a multi degree of freedom. C_1 is the modification factor for converting the calculated displacements from the linear elastic response to the expected maximum inelastic displacements. C_2 is the modification factor to represent the effect of hysteresis shape on the maximum displacement response. The value of this coefficient is determined according to structural performance level, the type of frame and the period of the structure. The C_3 is the modification factor to account for the increase in displacement due to the dynamic effects of P-Delta. T_e is the effective fundamental period. S_a is the spectral response acceleration vs structural period domain, and it is calculated as follows:

$$S_a = \begin{cases} \left(\dfrac{S_{XS}}{B_S}\right)\left(0.4 + 3\,T/T_0\right) & \text{for } \ 0 < T < 0.2T_0 \\ \dfrac{S_{XS}}{B_S} & \text{for } \ 0.2T_0 < T < T_0\,, \\ \left(S_{X1}/\left(B_1 T\right)\right) & \text{for } \ T > T_0 \end{cases} \tag{5}$$

where T is the elastic fundamental period of the structure that is obtained here from modal analysis of the structure.

T_0 is given by Eq. (6), where B_S and B_1 in accordance with Table 2-15 of the FEMA 273 are assumed as 1.

$$T_0 = \left(S_{X1}/B_S\right)/\left(S_{XS}/B_1\right), \tag{6}$$

where S_{XS} is the design short- period spectral response acceleration parameter and S_{X1} is the design spectral response acceleration parameter at one second that are expressed as:

$$S_{XS} = F_a S_S\,, \tag{7}$$

$$S_{X1} = F_v S_1\,. \tag{8}$$

Here F_a and F_v are site coefficients determined from FEMA-273, and the values of the response acceleration parameters S_S and S_1 obtained from Table 1 [27].

Table 1 The site parameters in the performance levels [27]

Hazard level	S_S (g)	S_1 (g)	F_a	F_v	T_0
10 %/50-years	1.587	0.560	1.00	1.50	0.529

The computational automatic procedure for performance-based optimal seismic design are shown in Fig. 1.

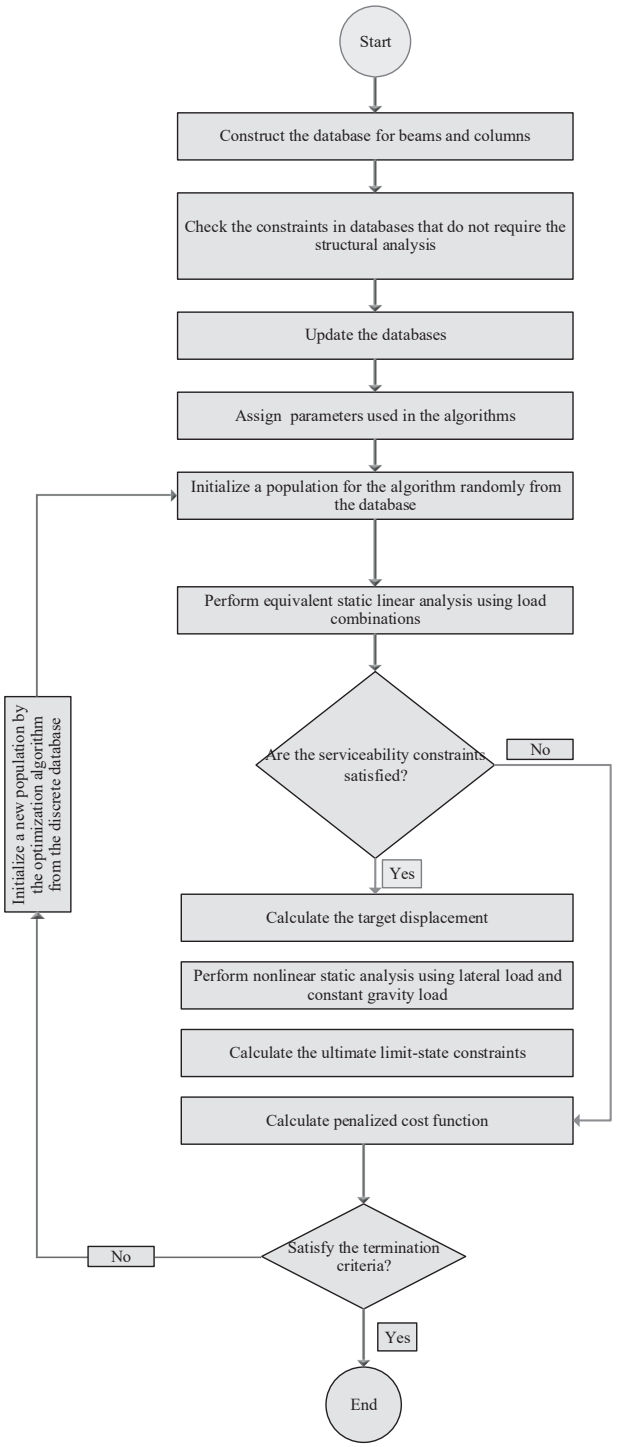

Fig. 1 The procedure of the PBOSD by the algorithms

2.2 Design variables and specifying database for sections

The design variables during the optimization process consist of the depth and width of the cross-section of columns and depth of beam elements, diameter of longitudinal bars, and number of bars. The bounds of the variables are shown in Table 2.

The variables are formulated in discrete form and two section databases for beams and columns are created. The ratio of depth to width of beam sections is varied between 1 and 3. In order to evaluate the flexural response of beams, the moment resisting capacity is calculated as Eq. (9) and saved in database:

$$M_n = A_s f_y (d - \frac{a}{2}), \tag{9}$$

where A_s is the total area of tensile reinforcing bars, f_y is the yield strength of bars, d is the distance from the edge of the section to the centroid of tension reinforcing bars, and a is the depth of the equivalent rectangular stress block defined as:

$$a = \frac{A_s f_y}{0.85 f_c' b}. \tag{10}$$

Here, f_c' is the compressive strength of the concrete and b is the width of the cross sections.

For column sections, in addition to variables, the parameters related to the *P-M* interaction diagram, as show in Fig. 2, are calculated according to the ACI code and saved in database. In the sections the rebars are distributed in all faces according of patterns shown in Fig. 3. The rebars are symmetric about the axis of bending and are the same size in each section. The total area for the *P-M* interaction diagram of the sections is calculated, and the sections are stored in their ascending order.

2.3 Objective functions

In this work, the aim of optimization is to minimize the construction cost and the amount of CO_2 emissions, as expressed by Eq. (11). In which n_b and n_c are the number of beams and columns, respectively; b_i, h_i, and A_{si} and L_i are the width, depth of the sections, area of the bars, and the length of the beams and columns, respectively; t_i is the thickness of the slab that is considered to be 290 mm. C_c, C_s, C_f and C_t are the unit rate of concrete, bars, form work, and scaffolding, respectively and their values are shown in Table 3. The parameter γ_s is unit weight of steel as 7849 kg/m^3.In the objective function of CO_2 emission, scaffolding is not considered.

Table 2 Parameters of the search space

		Width (mm)	Depth (mm)	Number of bars	Bar size
Column	Min	250	250	4	3
	Max	1200	1200	12	11
	Increment	50	50	2	1
Beam	Min	350	350	2	3
	Max	350	1050	5	11
	Increment		50	1	1

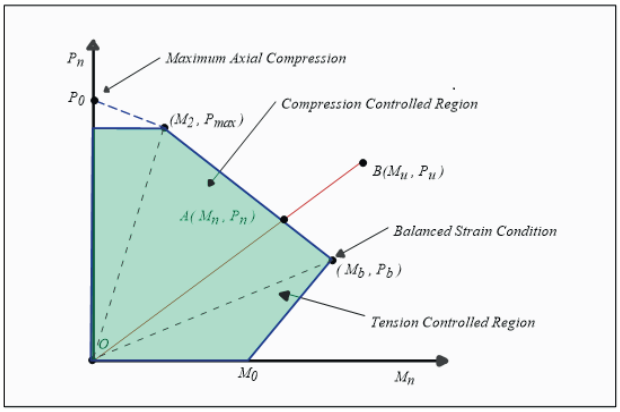

Fig. 2 Column load-moment interaction diagram

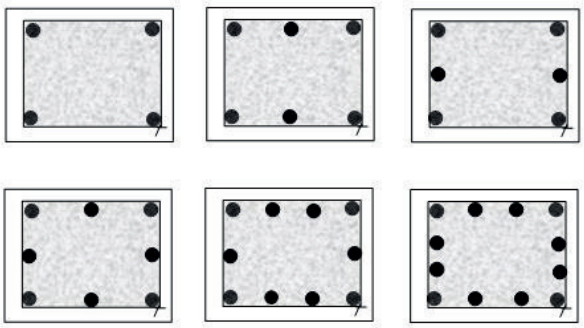

Fig. 3 Column reinforcement layouts

$$f_k = \sum_{i=1}^{n_b+n_c} \{C_c b_i h_i + C_s \gamma_s A_{si}\} L_i + \sum_{i=1}^{n_b} \{C_f (b_i + 2(h_i - t_i)) + C_t b_i\} L_i + \sum_{i=1}^{n_c} \{2C_f (b_i + h_i)\} L_i \tag{11}$$

2.4 Design constraints

According to design codes, serviceability and ultimate limit states structural constraint should be checked during the design process. Equivalent static analysis performed for structures and the serviceability constraints are checked according ACI code, then ultimate limit states

Table 3 Unit prices and CO_2 emissions [16]

Description	unit	Cost (€)		CO_2 (kg)	
		Beam	Column	Beam	Column
Steel B-500	kg	1.3	1.3	3.01	3.01
Concrete (40 MPa)	m^3	105.93	105.17	143.77	143.77
Concrete (25 MPa)	m^3	78.4	77.8	132.88	132.88
Form work	m^2	25.05	22.75	3.13	8.9
Scaffolding	m^2	38.89	-	-	-

constraints that are related to the maximum inter-story drift checked under pushover analysis in the performance level according FEMA code. In Eq. (12) the parameters g_i, x and n are the penalty of the ith constraint, elements and number of constraints, respectively. Furthermore f_p is the penalized objective function, f is the value of the objective function. In this study k is considered as 1.5.

$$f_p(x) = f \times (1 + \sum_{i=1}^{n} \max(0, g_i(x)))^k \tag{12}$$

2.4.1 Serviceability constraint

Constraints of the beams

For evaluating the moment capacity of the reinforced concrete beams, penalty function is calculated as Eq. (13). This restraint should be individually checked in areas that the positive and negative bending moment is maximum.

$$g_1 = \frac{|M_u| - \varnothing M_n}{\varnothing M_n}, \tag{13}$$

where M_u is the applied ultimate bending moment under applied loading, $\varnothing$ is the strength reduction factor which is equal to 0.9. M_n is the nominal bending moment capacity of the RC beams that is defined by Eq. (9).

According of ACI code, the ratio of minimum and maximum reinforcement of the beam sections are limited. The penalty of this constraints are as follows:

$$\rho_{min} = \frac{\sqrt{f_c'}}{4 f_y} \geq \frac{1.4}{f_y}, \quad g_2 = \rho_{min} - \rho \,. \tag{14}$$

$$\rho_{max} = 0.85 \beta_1 \frac{f_c'}{f_y} \frac{600}{600 + f_y}, \quad g_3 = \rho - \rho_{max} \,. \tag{15}$$

In order to control the deflection of the beams, the following penalty is considered in this study.

$$h_{min} = \frac{L}{21}, \quad g_4 = \frac{h_{min} - h}{h_{min}} \tag{16}$$

In the section of beams, if the effective depth (d) is less than the height of the compressive stress-block (a), the penalty will be defined as:

$$g_5 = \frac{a - d}{d} \,. \tag{17}$$

The minimum distance between bars are limited, where the penalty of this constraint is defined as:

$$g_6 = \frac{s_{min} - s}{s_{min}}, \qquad s_{min} = \max(d_b, 1 \ inch) \,. \tag{18}$$

Constraint of columns

When the combination of (M_u, P_u) under the applied loads falls inside the interaction *P-M* diagram, a column sections is suitable. The penalty function for the capacity of the column can be expressed as:

$$g_7 = \frac{l}{l_0} - 1 \,. \tag{19}$$

Based on Fig. 2, l is the distance between the origin of the interaction diagram (O) and the point indicating the position of combination (M_u, P_u) (B), and is the radial distance between the origin of the interaction diagram (O) and the point (A) indicates the intersection point of the vector l with the interaction curve.

The total area of bars (A_s) in the cross-section of reinforced concrete column is limited between 1 % and 8 % of the gross section (A_g). The penalty of minimum and maximum reinforcement for the columns is expressed as:

$$g_8 = \frac{0.01 \times A_g}{A_s} - 1 \leq 0 \,, \tag{20}$$

$$g_9 = \frac{A_s}{0.08 \times A_g} - 1 \leq 0 \,. \tag{21}$$

The function penalty defined for the distance between longitudinal bars is defined as:

$$g_{10} = \frac{s_{min} - s}{s_{min}}, \qquad s_{min} = max(1.5 d_b, \ 1.5 \ inch) \tag{22}$$

The dimensions of columns in each story should be smaller or equal than the dimensions of columns in bottom story, so the constraints are expressed as follow:

$$g_{11} = \frac{b_T}{b_B} - 1 , \tag{23}$$

$$g_{12} = \frac{h_T}{h_B} - 1 , \tag{24}$$

where B and T represent the bottom column and the top column, b and h are the width and depth of the column cross section, respectively.

2.4.2 Ultimate limit-state constraint

Lateral drift is an important indicator for measuring the damage in structures and should be controlled in seismic design [28]. Performance-based constraint are expressed as lateral drift at the performance level as follows:

$$g_{13} = \frac{\theta_{max}^{LS}}{\theta_{allow}^{LS}} - 1 , \tag{25}$$

where θ_{max}^{LS} are maximum inter-story drift of the frame and θ_{allow}^{LS} are allowable drifts that are chosen 2 % according to FEMA-273.

2.5 Structural analysis model

Linear static analysis and nonlinear static analysis of the structures are performed in the finite element software OpenSees [29] and the response of the elements are obtained. The limitations of the ACI 318-08 code, FEMA and the optimization algorithm are handled in MATLAB [30] software. In linear static analysis, the beams and columns are modeled with *elastic beam-column element* and in nonlinear static analysis *nonlinear beam column-element* with distributed plasticity are used to model of beams and columns. Nonlinear concrete and steel material properties are provided in Table 4. As it is mentioned in Table 4, the effects of confinement and unconfined parts of the fiber section are imposed in the definition of concrete properties. Also, the P-Delta effects are considered as a geometric transformation. Thus, both material and geometry nonlinearity are considered.

3 Optimization algorithm

The Colliding Bodies Optimization (CBO) algorithm was developed by Kaveh and Mahdavi [31]. This algorithm is inspired by the laws of momentum and energy of the physics. To obtain reliable solutions and fast convergence, Kaveh and Ilchi Ghazaan [32] has been developed the enhanced colliding bodies optimization (ECBO) algorithm. A comparative study of these algorithms can be found in Kaveh and Ilchi Ghazaan [33]. The procedure of the ECBO algorithm can be expressed as:

Step 1: Initial position of each colliding bodies is randomly obtained in the search space as follows:

$$x_i^0 = x_{min} + rand\left(x_{max} - x_{min}\right), \quad i = 1,2,\ldots,n , \tag{26}$$

where x_i^0 is the initial position of the ith CB, x_{max} and x_{min} are the minimum and the maximum allowable values of variables, respectively. The *rand* parameter is a random value in the range [0, 1] and n is the number of CB.

Step 2: In the next step, the mass of each object is determined as follows:

$$m_k = \frac{\frac{1}{fit(k)}}{\sum_{i=1}^{n} \frac{1}{fit(i)}}, \quad k = 1,2,\ldots,n , \tag{27}$$

where $fit(i)$ represents the objective function value of the ith colliding body and n is the number of populations.

Step 3: Colliding Memory (CM) is utilized to save a number of historically best CB vectors and their related mass and objective function values. Solution vectors which are saved in CM are added to the population and the same number of current worst CBs are deleted.

Table 4 The properties of materials

Concrete (uniaxial material concrete01)					
Material type		f_c' (MPa)	ε_{c0}	f_{cu}' (MPa)	ε_{cu}
Concrete (40 MPa)	Core concrete of beams (confined)	44	0.00296	15.3	0.0148
	Core concrete of columns (confined)	48	0.0032	16.8	0.048
	Cover concrete (unconfined)	40	0.0025	14	0.0055
Concrete (25 MPa)	Core concrete of beams (confined)	27.5	0.0025	9.6	0.011
	Core concrete of columns (confined)	30	0.0025	10.5	0.038
	Cover concrete (unconfined)	25	0.0025	8.75	0.0055
Steel (Uniaxial Material Steel01)					
Material type			f_c' (MPa)	E_0	b
Reinforcing steel			500	2e5	0.01

Step 4: Objects are arranged in descending order and are divided into two equal groups of stationary and moving objects. To improve the position of moving objects and move stationary objects toward a better position, the moving object moves toward a stationary object and a collision occurs, Fig. 4.

Step 5: The velocity of stationary objects before collision is zero and the velocity of moving objects before collision is calculated as follows:

$$v_i = 0, \quad i = 1,2,\ldots,\frac{n}{2} \tag{28}$$

$$v_i = x_{i-\frac{n}{2}} - x_i, \quad i = \frac{n}{2}+1,...,n \tag{29}$$

Step 6: After the collision of the moving and stationary objects, velocity of the objects is calculated as follows:

Stationary objects:

$$v_i^{'} = \frac{(m_{i+\frac{n}{2}} + \varepsilon m_{i+\frac{n}{2}})v_{i+\frac{n}{2}}}{m_i + m_{i+\frac{n}{2}}}, \quad i = 1,2,\ldots,\frac{n}{2}. \tag{30}$$

Moving objects:

$$v_i^{'} = \frac{\left(m_i - \varepsilon m_{i-\frac{n}{2}}\right)v_i}{m_i + m_{i-\frac{n}{2}}}, \quad i = \frac{n}{2}+1,\ldots,n. \tag{31}$$

Coefficient of Restitution (ε) is defined as:

$$\varepsilon = 1 - \frac{iter}{iter_{max}}. \tag{32}$$

Step 7: Using the generated velocities after the collision and their old position, the new positions of the objects for both groups are updated as follows:

The new position of moving object:

$$x_i^{new} = x_{i-\frac{n}{2}} + rand^{\circ}v_i^{'}, \quad i = \frac{n}{2}+1,\frac{n}{2}+2,\ldots,n. \tag{33}$$

In which x_i^{new} is the new position of the *i*th CBs and *rand* is a random vector uniformly distribution in the range (–1, 1). v_i' is the velocity of *i*th CB after collision. The sign "°" denotes an element-by-element multiplication.

The new position of stationary object:

$$x_i^{new} = x_{i-\frac{n}{2}} + rand^{\circ}v_i^{'}, \quad i = \frac{n}{2}+1,\frac{n}{2}+2,\ldots,n. \tag{34}$$

Step 8: The *Pro* parameter is compared with the random number rn_i(i = 1, 2…, n), If $Pro > rn_i$, a CB is randomly selected from both moving and stationary groups and one related component regenerate.

Step 9: Return to Step 2 until terminating criterion is satisfied.

Further explanations on CBO and ECBO and other applications can be found in Kaveh [34, 35] and Kaveh and Bakhshpoori [36].

4 Numerical example

A four-story reinforced concrete frame is considered to investigate the main aim of this paper. The height of each story is 3 meters and the length of each span is 10 meters. The geometry and grouping of members are shown in Fig. 5. The frame consists of 8 column groups and 4 groups of beams. The procedure described in Section 2 for performance-based optimum seismic design, is used to minimize the cost and carbon dioxide emissions. The frame optimally designed for three ductility classes (high ductility DCH, medium DCM and low DCL), for two various PGA (0.2 g, 0.35 g) and concrete classes (f_c = 25 MPa, f_c = 40 MPa). According to the Iranian seismic resistant design-2800 code, the behavior factor for the high to low classes of ductility is 7.5, 5 and 3 respectively. In all cases, the yield strength of reinforcing steels is 500 MPa. It should be noted that the addition of transverse reinforcement to achieve higher ductility capacity for high and medium ductility classes does not significantly increase the CO_2 emissions and the optimal cost. This is due to their lower contribution in the cost and total CO_2 emissions [22]. Therefore, in this study, only the effect of behavior factor R has been investigated for all ductility classes. In the following, the evaluation of design factors and results of their optimally designs are given comparatively.

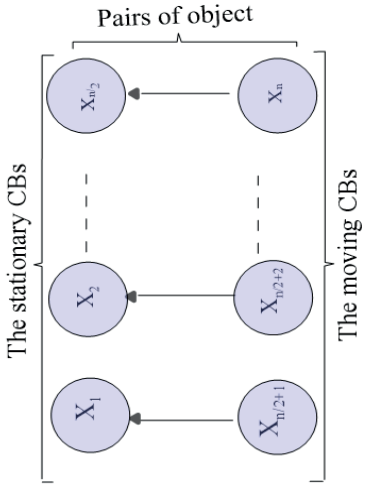

Fig. 4 The pairs of objects for collision

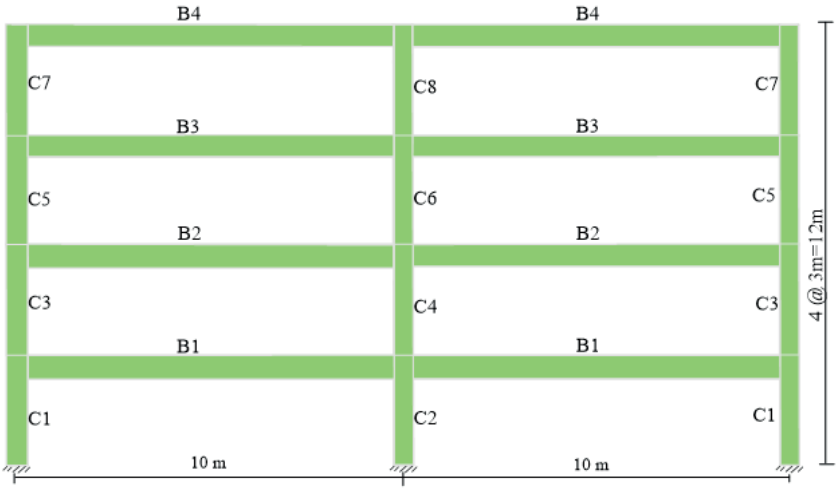

Fig. 5 Geometry and grouping of the elements for the considered RC frame

4.1 Ductility classes and the relationship between optimal cost and optimal CO_2 emissions

Case I: In this case the frame is optimally designed for the low, medium and high ductility classes. Where the PGA is 0.35 g and compression strength of concrete (f_c) is 40 MPa. Fig. 6 shows the amount of optimal cost and optimal carbon dioxide emissions. With increasing levels of ductility from DCL to DCM, the cost and CO_2 emissions reduce 10 % and 11 % respectively. But the reduction of cost and CO_2 emissions from DCM to DCH is 5.3 % and 5.2 % respectively. Fig. 7 shows the convergence curve for the lowest cost and lowest CO_2 emissions. Fig. 8 also shows the relationship between optimal cost and optimal carbon dioxide emissions. At the DCL ductility level, when the objective function is to minimize carbon dioxide emissions, increasing the optimal cost can significantly reduce CO_2 emissions, but at the DCH and DCM levels to reduce CO_2, the increase of cost is significant.

Case II: In this case, the methodologies of seismic design are the same as the frame in Case I, with the difference that in this case, concrete with a compressive strength of 25 MPa has been used. Fig. 9 shows the amount of optimal cost and optimal carbon dioxide emissions. With increasing the levels of ductility from DCL to DCM, there will be a significant reduction in the cost and carbon dioxide emissions, but this reduction is smaller than DCM to DCH. Fig. 10 shows the convergence curves for the lowest cost and lowest CO_2 emissions. Fig. 11 also shows the relationship between optimal cost and optimal carbon dioxide emissions. In this case, as in the Case I, at the DCL ductility level, when the objective function is to minimize the carbon dioxide emissions, increasing the optimal cost can significantly reduce CO_2 emissions, but at the DCH and DCM levels to reduce CO_2, the increase of cost is high.

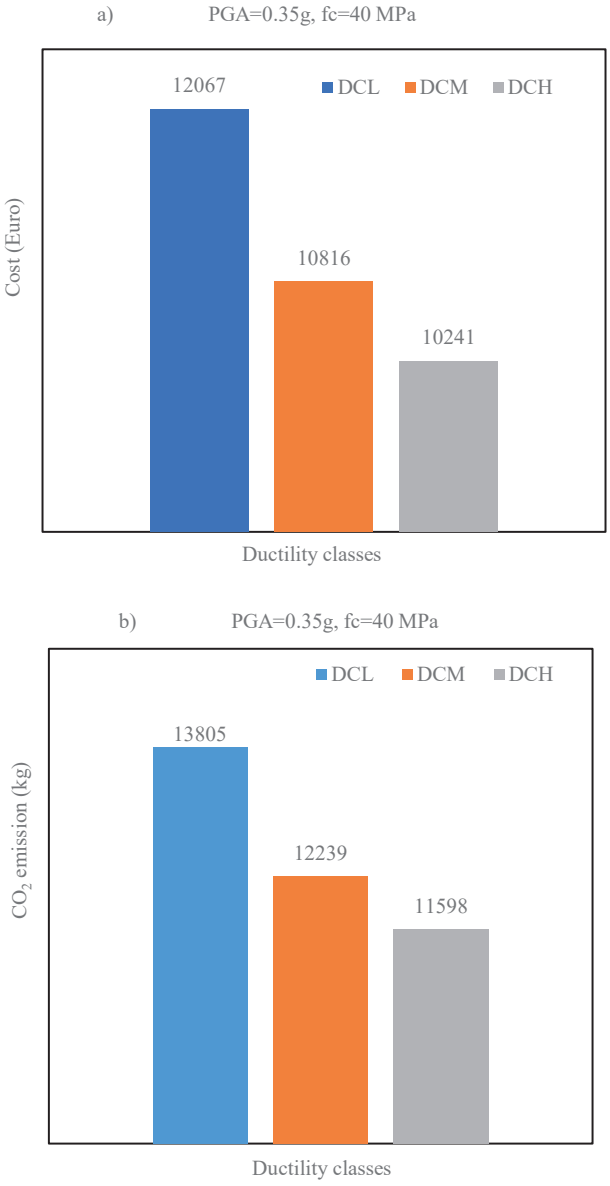

Fig. 6 Optimal solutions of the frame for different ductility classes in the Case I; a) Optimum cost; b) Optimum CO_2 emissions

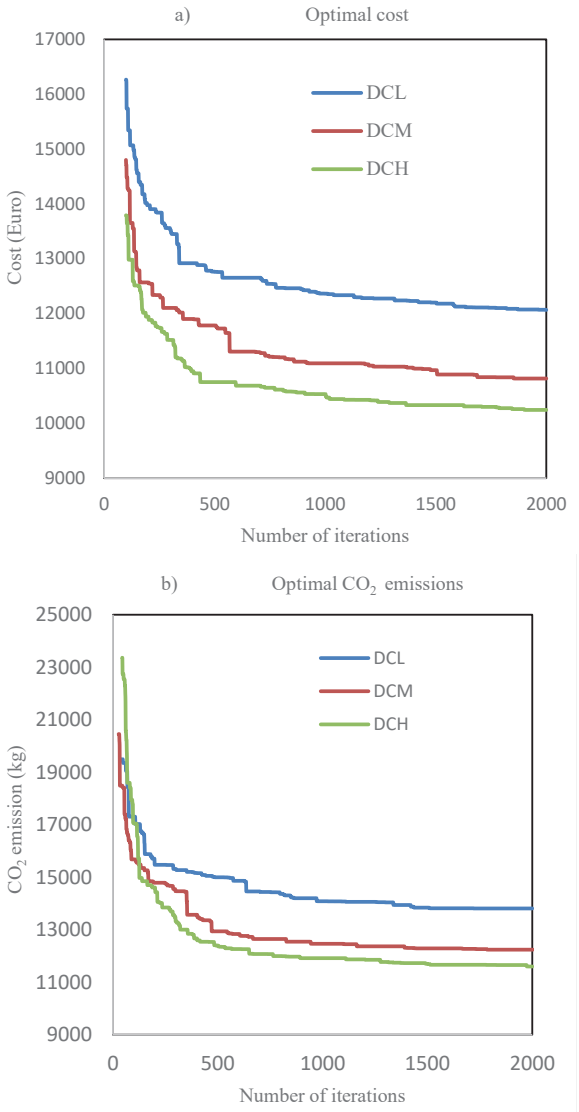

Fig. 7 Convergence curves of the frame for the Case I; a) for lowest cost; b) for the lowest CO_2 emission

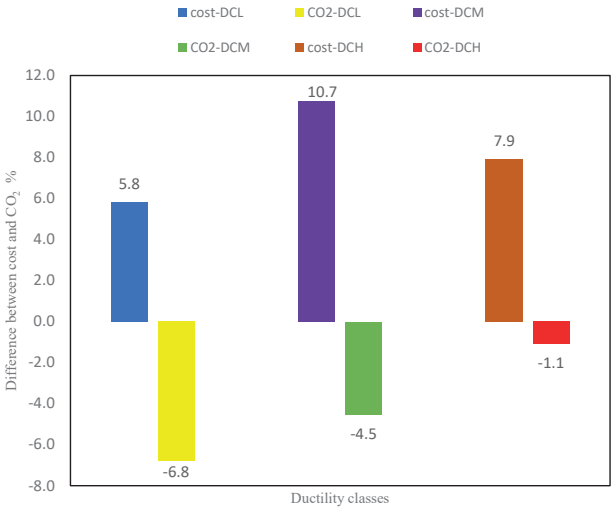

Fig. 8 Relationship between the minimum cost and minimum CO_2 emissions of the frame in the Case I

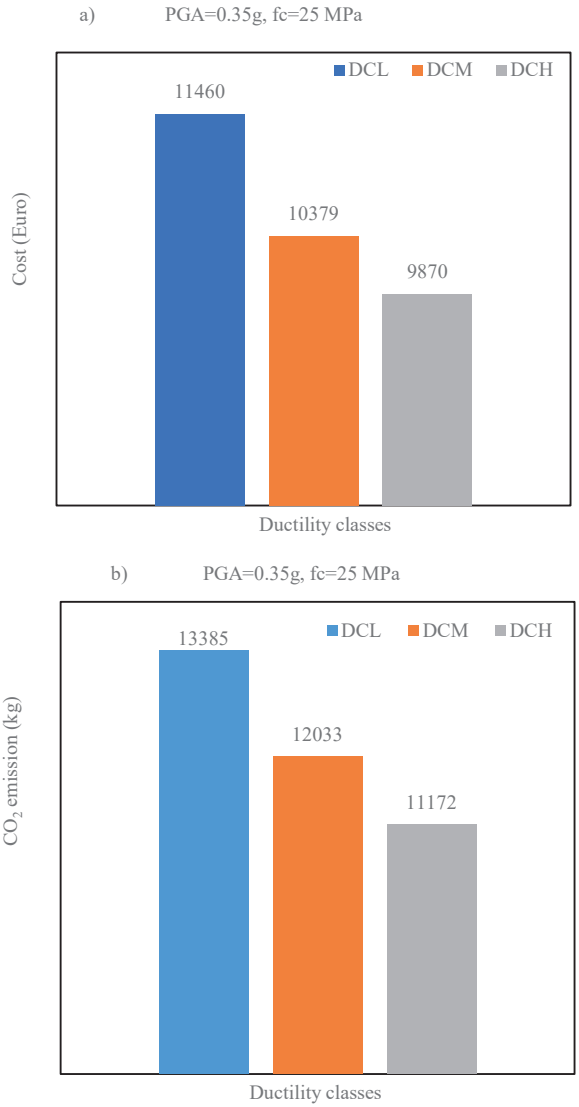

Fig. 9 Optimal solutions of the frame for different ductility classes in the Case II; a) Optimum cost; b) Optimum CO2 emissions

Case III: In this case, the frame is optimally designed for all three classes of ductility. In all cases, the PGA is 0.2 g and the compressive strength of concrete is 25 MPa. Fig. 12 and Fig. 13 show that by increasing the levels of ductility from DCL to DCM, the cost and carbon dioxide emissions can be reduced, however the result of the DCM is almost same as the result of DCH. In Fig. 14, the relationships between optimal cost and optimal carbon dioxide emissions are shown.

4.2 Concrete class

In this section, the effect of compression strength of concrete on the optimal cost and optimal CO_2 emissions in different ductility classes are evaluated. Fig. 15 shows the comparative result of frame in Case I and Case II, where the compression strength of concrete is 40 MPa and 25 MPa,

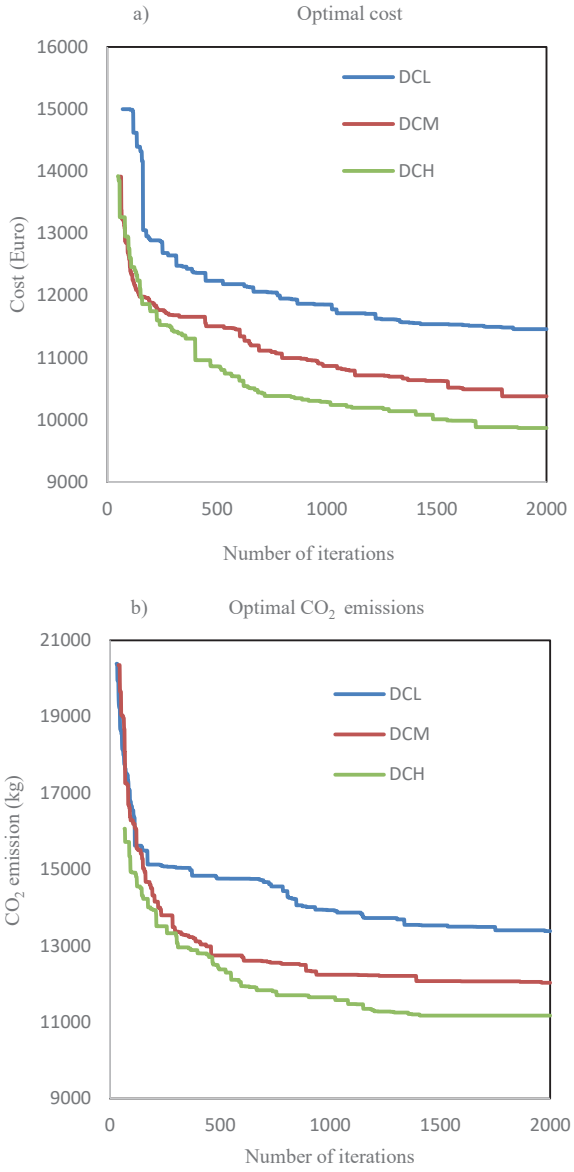

Fig. 10 Convergence curves of the frame in the Case II; a) for lowest cost; b) for the lowest CO_2 emission

respectively. It can be concluded that the use of concrete with high compression strength, increases the capacity of the members of the structure, however, the amount of optimal cost and optimal CO_2 emissions in these types of structures is more. It should be noted that according to Table 3, higher concrete class produces higher costs and CO_2 emissions than lower concrete class.

4.3 Peak Ground Acceleration

In this section, the effect of PGA design on the optimal cost and optimal CO_2 emissions in the three ductility classes are evaluated. The comparative results of the solutions in case II and case III that are obtained for two seismic levels of PGA: 0.35 g, 0.2 g are given in Fig. 16. It is

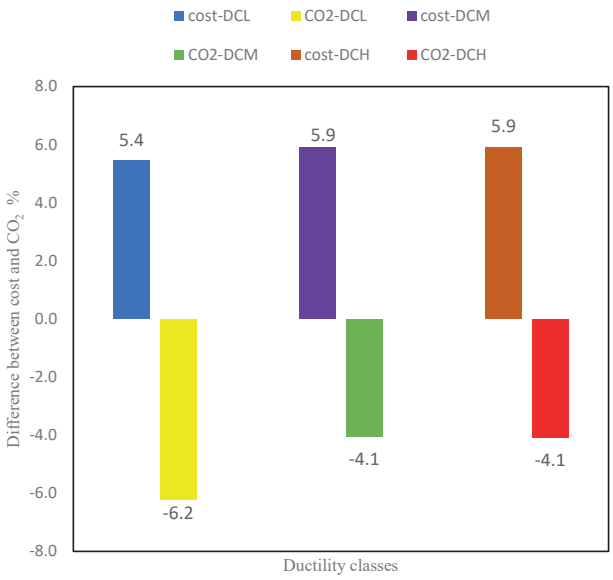

Fig. 11 Relationship between minimum cost and minimum CO_2 emissions of frame in in the Case II

concluded that by reducing the PGA design, the optimal cost and optimal carbon dioxide emissions can be reduced, which has a significant effect on the low ductility level.

5 Conclusions

The construction industry has a remarkable contribution in the production of greenhouse gases. Researchers have used the methods to reduce the CO_2 emissions from construction. One of these methods is the use of optimization methods in structural design stage. In limited studies of optimization, nonlinear analysis is used for structural analysis and controlling the ultimate limit states constraint. In this study, under nonlinear structural analysis, the effect of design factors on the relationship between optimal cost and carbon dioxide emission of the RC frames is studied and the important parameters in minimizing CO_2 emissions are identified. The parameters are different classes of ductility, peak ground accelerations and different types of concrete class. Nonlinear static analysis (pushover) has been used for structural analysis. In addition to controlling serviceability constraints under equivalent static linear analysis, inter-story drift constraints are also controlled under nonlinear static analysis. The frames are optimally designed according to the ACI 318-08 and FEMA codes. Here the aim of the optimization was to minimize economic costs and CO_2 emissions. The ECBO algorithm has been used to obtain optimal solutions. It is concluded that by changing the design methodology from DCL to DCM, the amount of optimal cost and optimal CO_2 emissions can be decreased significantly, but the difference of the optimal results from

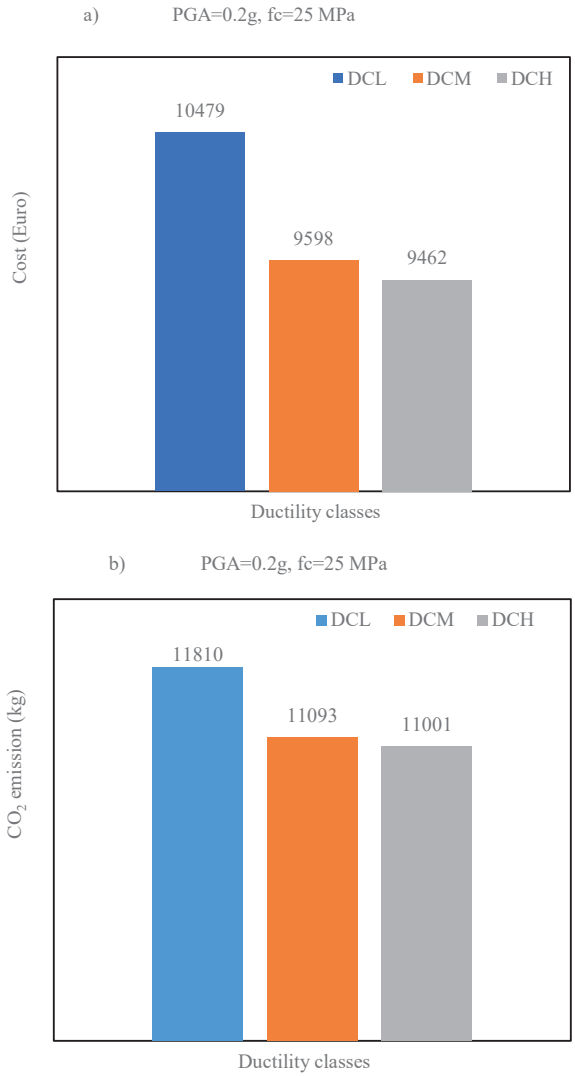

Fig. 12 Optimal solutions of frame for the different ductility classes in the Case III; a) Optimum cost; b) Optimum CO_2 emissions

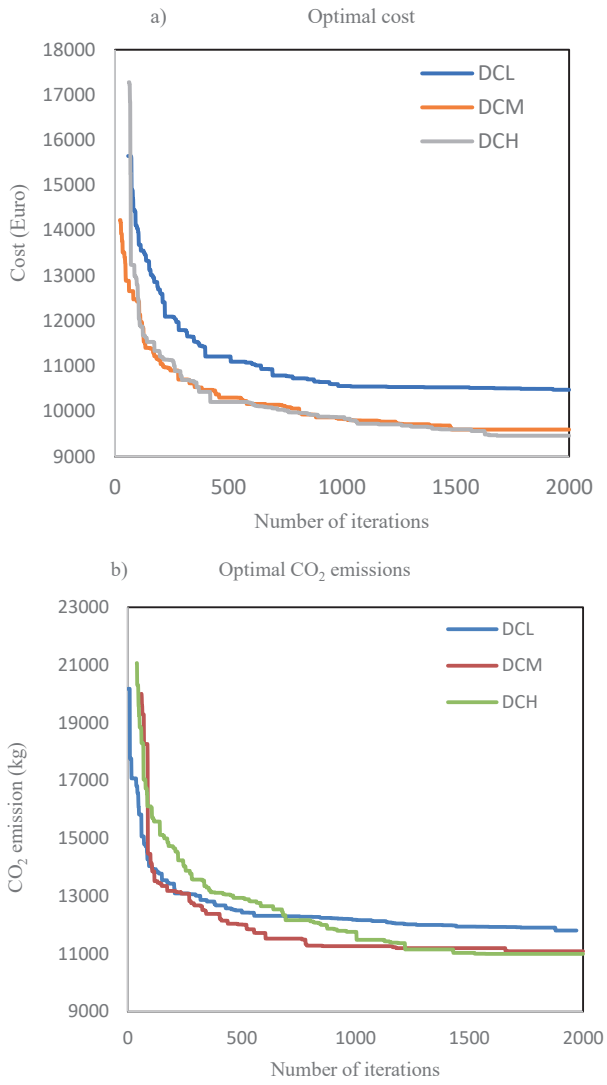

Fig. 13 Convergence curves of the frame in the Case III; a) for lowest cost; b) for the lowest CO_2 emission

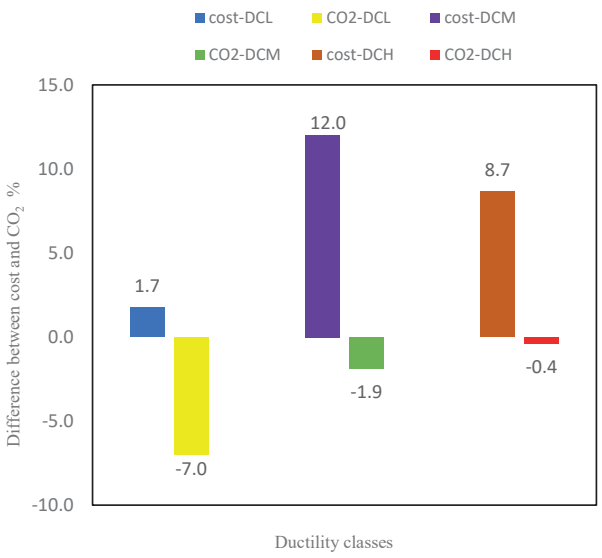

Fig. 14 Relationship between the minimum cost and minimum CO_2 emissions of frame in in the Case III

DCM to DCH are small. Meanwhile, the relationship between optimal objects shows that in the low ductility class, with increasing the percentage of optimal cost can be greatly reduced the carbon dioxide emissions. But in the high and medium ductility class, a large percentage of the cost must be increased to reduce CO_2. Although the use of high concrete class increases the capacity of the structure, it also slightly increases the cost and optimal value of the CO_2 emissions. This is due to the higher unit cost and CO_2 emissions. The design of structures in low seismic areas produces lower costs and CO_2 emissions. In other words, by reducing the PGA design, the optimal cost and optimal carbon dioxide emissions can be reduced, which has a significant effect on the possibility of choosing low ductility level.

Conflict of interest

No potential conflict of interest was reported by the authors.

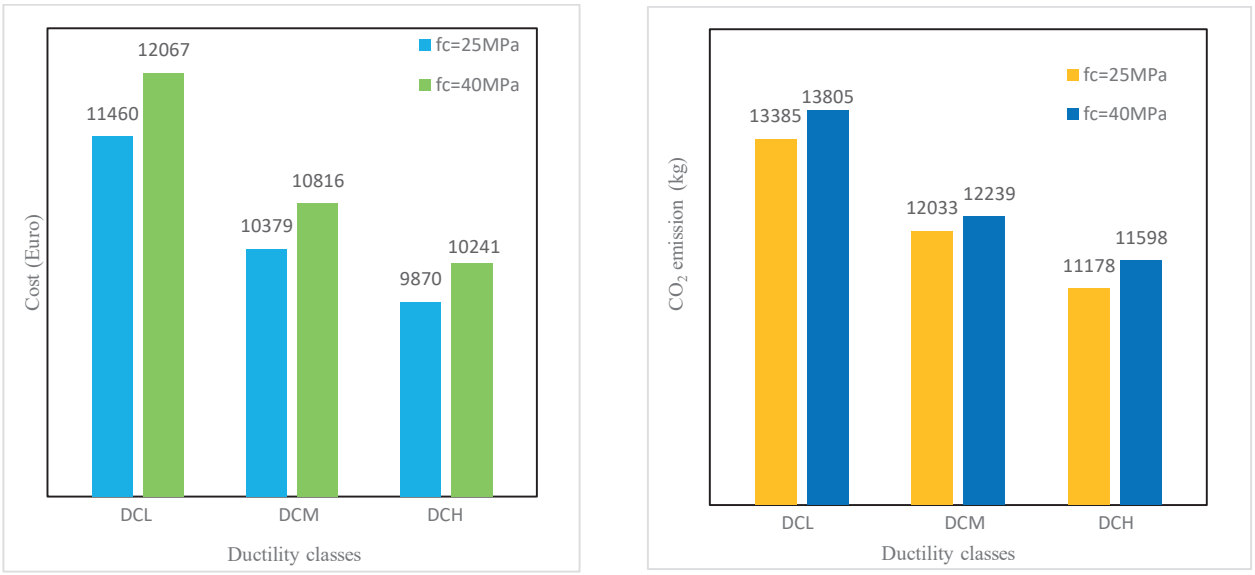

Fig. 15 Optimal cost and optimal CO_2 emissions for different concrete classes

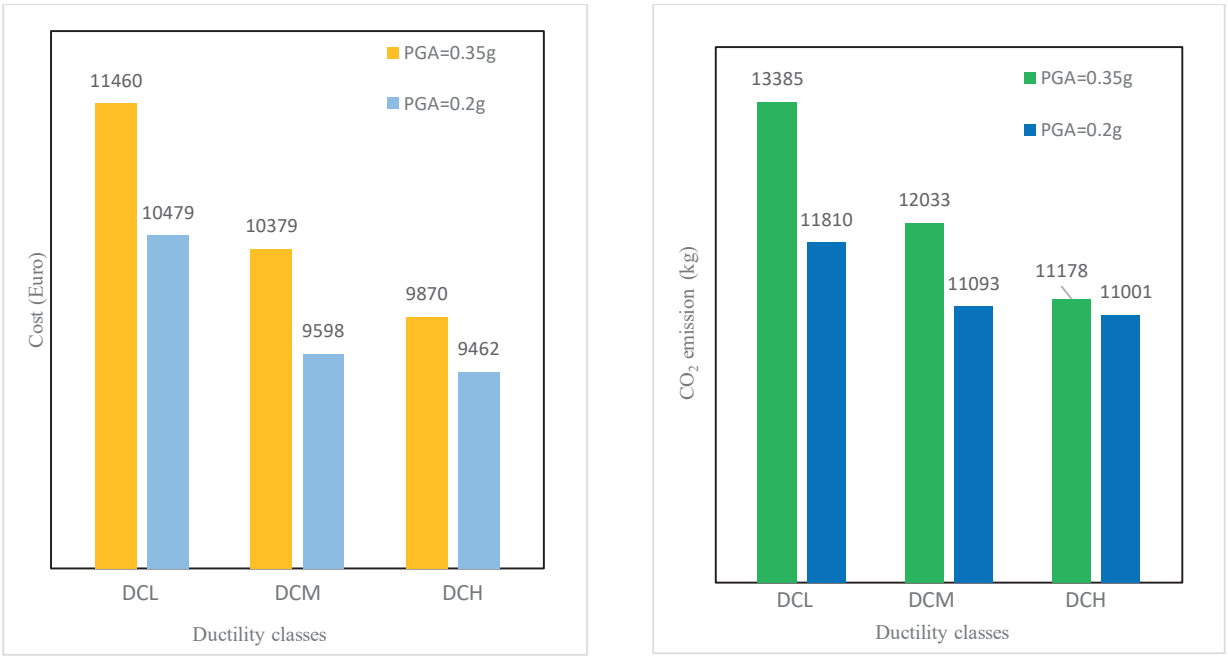

Fig. 16 Optimal cost and optimal CO_2 emissions for different PGA design

References

[1] Kaveh, A., Kabir, M. Z., Bohlool, M. "Optimal Design of Multi-Span Pitched Roof Frames with Tapered Members", Periodica Polytechnica Civil Engineering, 63(1), pp. 77–86, 2019. https://doi.org/10.3311/PPci.13107

[2] Hasançebi, O., Kazemzadeh Azad, S. "Discrete Sizing of Steel Frames Using Adaptive Dimensional Search Algorithm", Periodica Polytechnica Civil Engineering, 63(4), pp. 1062–1079, 2019. https://doi.org/10.3311/PPci.14746

[3] Kaveh, A., Mahdavi, V. R., Kamalinejad, M. "Optimal Design of the Monopole Structures Using the CBO and ECBO Algorithms", Periodica Polytechnica Civil Engineering, 61(1), pp. 110–116, 2017. https://doi.org/10.3311/PPci.8546

[4] Kaveh, A., Sabzi, O. "A comparative study of two meta-heuristic algorithms for optimum design of reinforced concrete frames", International Journal of Civil Engineering, 9(3), pp. 193–206, 2011. [online] Available at: http://ijce.iust.ac.ir/article-1-477-en.html

[5] Tapao, A., Cheerarot, R. "Optimal parameters and performance of artificial bee colony algorithm for minimum cost design of reinforced concrete frames", Engineering Structures, 151, pp. 802–820, 2017. https://doi.org/10.1016/j.engstruct.2017.08.059

[6] Akin, A., Saka, M. P. "Harmony search algorithm based optimum detailed design of reinforced concrete plane frames subject to ACI 318-05 provisions", Computers and Structures, 147, pp. 79–95, 2015. https://doi.org/10.1016/j.compstruc.2014.10.003

[7] Esfandiari, M. J., Urgessa, G. S., Sheikholarefin, S., Dehghan Manshadi, S. H. "Optimum design of 3D reinforced concrete frames using DMPSO algorithm", Advances in Engineering Software, 115, pp. 149–160, 2018. https://doi.org/10.1016/j.advengsoft.2017.09.007

[8] Kaveh, A., Izadifard, R. A., Mottaghi, L. "Cost Optimization of RC Frames Using Automated Member Grouping", International Journal of Optimization in Civil Engineering, 10(1), pp. 91–100, 2020. [online] Available at: http://ijoce.iust.ac.ir/article-1-422-en.html

[9] Gharehbaghi, S., Moustafa, A., Salajegheh, E. "Optimum seismic design of reinforced concrete frame structures", Computers and Concrete, 17(6), pp. 761–786, 2016. https://doi.org/10.12989/cac.2016.17.6.761

[10] Duxson, P., Provis, J. L., Lukey, G. C., van Deventer, J. S. J. "The role of inorganic polymer technology in the development of 'green concrete' ", Cement and Concrete Research, 37(12), pp. 1590–1597, 2007. https://doi.org/10.1016/j.cemconres.2007.08.018

[11] Gartner, E. "Industrially interesting approaches to 'low-CO_2' cements", Cement and Concrete Research, 34(9), pp. 1489–1498, 2004. https://doi.org/10.1016/j.cemconres.2004.01.021

[12] Eleftheriadis, S., Duffour, P., Greening, P., James, J., Stephenson, B., Mumovic, D. "Investigating relationships between cost and CO_2 emissions in reinforced concrete structures using a BIM-based design optimisation approach", Energy & Buildings, 166, pp. 330–346, 2018. https://doi.org/10.1016/j.enbuild.2018.01.059

[13] Yoon, Y.-C., Kim, K.-H., Lee, S.-H., Yeo, D. "Sustainable design for reinforced concrete columns through embodied energy and CO_2 emission optimization", Energy & Buildings, 174, pp. 44–53, 2018. https://doi.org/10.1016/j.enbuild.2018.06.013

[14] de Medeiros, G. F., Kripka, M. "Optimization of reinforced concrete columns according to different environmental impact assessment parameters", Engineering Structures, 59, pp. 185–194, 2014. https://doi.org/10.1016/j.engstruct.2013.10.045

[15] Park, H. S., Lee, H., Kim, Y., Hong, T., Choi, S. W. "Evaluation of the influence of design factors on the CO_2 emissions and costs of reinforced concrete columns", Energy and Buildings, 82, pp. 378–384, 2014. https://doi.org/10.1016/j.enbuild.2014.07.038

[16] Camp, C. V., Huq, F. "CO_2 and cost optimization of reinforced concrete frames using a big bang-big crunch algorithm", Engineering Structures, 48, pp. 363–372, 2013. https://doi.org/10.1016/j.engstruct.2012.09.004

[17] Paya-Zaforteza, I., Yepes, V., Hospitaler, A., González-Vidosa, F. "CO_2-optimization of reinforced concrete frames by simulated annealing", Engineering Structures, 31(7), pp. 1501–1508, 2009. https://doi.org/10.1016/j.engstruct.2009.02.034

[18] Kaveh, A., Izadifard, R. A., Mottaghi, L. "Optimal design of planar RC frames considering CO_2 emissions using ECBO, EVPS and PSO metaheuristic algorithms", Journal of Building Engineering, 28, Article number: 101014, 2020. https://doi.org/10.1016/j.jobe.2019.101014

[19] Kaveh, A., Mottaghi, L., Izadifard, R. A. "Sustainable design of reinforced concrete frames with non-prismatic beams", Engineering with Computers, 2020. https://doi.org/10.1007/s00366-020-01045-4

[20] Kaveh, A., Ardalani, S. "Cost and CO_2 Emission Optimization of Reinforced Concrete Frames Using Enhanced Colliding Bodies Algorithm", Asian Journal of Civil Engineering, 17(6), pp. 831–858, 2016. [online] Available at: https://www.magiran.com/paper/1490806?lang=en

[21] Park, H. S., Hwang, J. W., Oh, B. K. "Integrated analysis model for assessing CO2 emissions, seismic performance, and costs of buildings through performance-based optimal seismic design with sustainability", Energy and Buildings, 158, pp. 761–775, 2018. https://doi.org/10.1016/j.enbuild.2017.10.070

[22] Mergos, P. E. "Seismic design of reinforced concrete frames for minimum embodied CO2 emissions", Energy and Buildings, 162, pp. 177–186, 2018. https://doi.org/10.1016/j.enbuild.2017.12.039

[23] BHRC "No. 2800, Iranian Code of Practice for Seismic Resistant Design of Buildings", Building and Housing Research Center, Tehran, Iran, 2007. (in Persian)

[24] ACI Committee 318 "Building Code Requirements for Structural Concrete (ACI 318-08) and Commentary", American Concrete Institute, Farmington Hills, MI, USA, 2008.

[25] FEMA "FEMA-273 NEHRP guideline for the seismic rehabilitation of buildings", Federal Emergency Management Agency, Washington, DC, USA, 1997.

[26] FEMA "FEMA-356 Prestandard and commentary for the seismic rehabilitation of buildings", Federal Emergency Management Agency, Washington, DC, USA, 2000.

[27] Fathali, M. A., Hoseini Vaez, S. R. "Optimum performance-based design of eccentrically braced frames", Engineering Structures, 202, Article number: 109857, 2020. https://doi.org/10.1016/j.engstruct.2019.109857

[28] Moehle. J. P., Mahin, S. A. "Observations on the Behavior of Reinforced Concrete Buildings During Earthquakes", In: Ghosh, S. K. (ed.) Earthquake-resistant Concrete Structures – Inelastic Response and Design SP127, American Concrete Institute, Farmington Hills, MI, USA, 1991, pp. 67–90. https://doi.org/10.14359/3007

[29] OpenSees "OpenSees Open System for Earthquake Engineering Simulation", Pacific Earthquake Engineering Research Centre, University of California, Berkeley, CA USA, 2012. [online] Available at: https://opensees.berkeley.edu

[30] Math Works "MATLAB", Math Works Inc, Natick, MA USA, 2016. [online] Available at: https://www.mathworks.com

[31] Kaveh, A., Mahdavi, V. R. "Colliding bodies optimization: A novel meta-heuristic method", Computers and Structures, 139, pp. 18–27, 2014. https://doi.org/10.1016/j.compstruc.2014.04.005

[32] Kaveh, A., Ilchi Ghazaan, M. "Enhanced colliding bodies optimization for design problems with continuous and discrete variables", Advances in Engineering Software, 77, pp. 66–75, 2014. https://doi.org/10.1016/j.advengsoft.2014.08.003

[33] Kaveh, A., Ilchi Ghazaan, M. "A comparative study of CBO and ECBO for optimal design of skeletal structures", Computers and Structures, 153, pp. 137–147, 2015. https://doi.org/10.1016/j.compstruc.2015.02.028

[34] Kaveh, A. "Advances in Metaheuristic Algorithms for Optimal Design of Structures", 2nd ed., Springer, Cham, Switzerland, 2017. https://doi.org/10.1007/978-3-319-05549-7

[35] Kaveh, A. "Applications of Metaheuristic Optimization Algorithms in Civil Engineering", Springer, Cham, Switzerland, 2017. https://doi.org/10.1007/978-3-319-48012-1

[36] Kaveh, A., Bakhshpoori, T. "Metaheuristics: Outlines, MATLAB Codes and Examples", Springer, Cham, Switzerland, 2019. https://doi.org/10.1007/978-3-030-04067-3